In the search for ditriel B□Al non-covalent bonding

Berski, S. and Gordon, A.

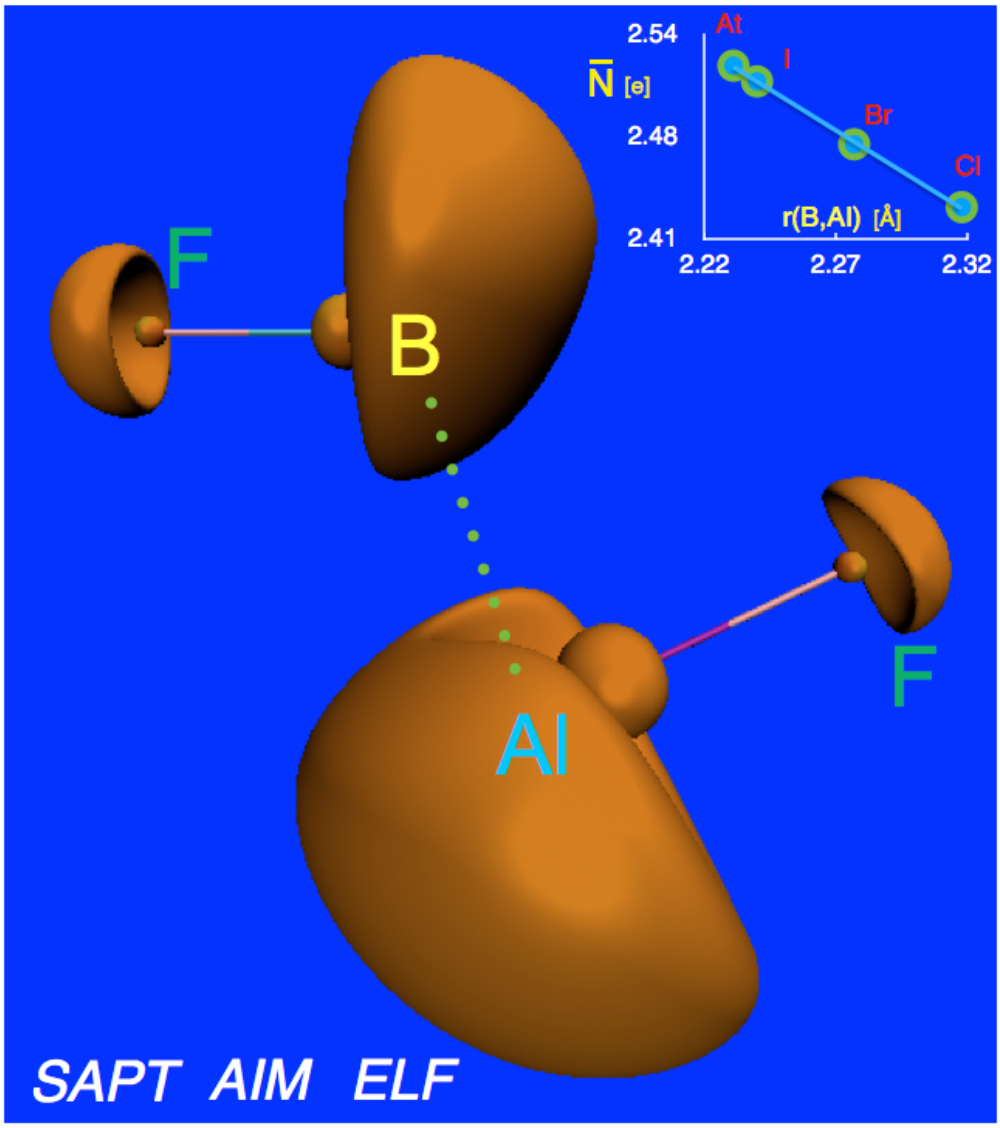

The ditriel B···Al interaction has been characterised using SAPT, AIM and ELF.

In the search for ditriel B···Al non-covalent bonding.

Slawomir Berski, Agnieszka J. Gordon

[1)] Faculty of Chemistry, University of Wroclaw, 14 F. Joliot-Curie, 50-383, Wroclaw, Poland. Tel: +48 (0)71 3757246 Fax: +48 (0)71 3282348

[a)] Corresponding author; email: **slawomir.berski@chem.uni.wroc.pl**

Keywords: triel bonding, chemical bond, boron, aluminium, BAl, topology, Electron Localization Function, ELF, AIM, Lewis structure

Abstract

The ditriel B···Al interaction has been characterised in the $F^{\delta-}B^{\delta+}\cdots Al^{\delta+}F^{\delta-}$ ($\delta > 0.6e$) molecule using CCSD(T)/aug-cc-pVTZ calculations. It has a non-covalent character as evidenced by the topological analysis of electron density (AIM) and electron localisation function (ELF) fields. The B···Al bonding is very weak (< 1 kcal/mol) and unique among the FBTF (T= B, Al, Ga, In) molecules. SAPT analysis shows that it has mainly an electrostatic character but the energetic stability of the molecule is gained at the second order of the perturbation expansion with the dispersion and induction energies. Substitution of the F atom by less electronegative atom such as Cl, Br, I and At results in shortening of the B···Al separation and creating XBAlX (X= Cl, Br, I, At) molecules with 2c-2e covalent B-Al bond. The topology of ELF for BF and AlF bonds reveals features, which may be explained evoking high electropositive character of the Al atom.

I. Introduction

A number of studies on non-covalent interactions has recently significantly increased. Non-covalent interactions are of importance in supramolecular chemistry [1], crystal engineering [2], catalysis [3], molecular machines [4], membrane ion transport [5]. A systematic nomenclature has been proposed, based on the main element of the donor-acceptor interaction acting as an electrophile [6]. Apart from widely known and well researched hydrogen bonds, there are alkali bonds, alkaline earth bonds, regium bonds, spodium bonds, triel bonds, tetrel bonds, pnictogen bonds, chalcogen bonds, halogen bonds, and aerogen bonds.

The triel bonding describes a non-covalent interaction between elements in Group 13 of the periodic table and atoms with 'abundant' electron density. There have been many theoretical publication on the triel interactions [7,8,9,10,11,12,13] where the concept of the σ-hole and π-hole [14] have been explored. However, studies on ditriel bonding, where two triel (T) atoms interact with each other in a non-covalent way appear to be scarce.

In order to gain better understanding of the nature of non-covalent interactions, the FBTF (T= B, Al, Ga, In) molecules have been theoretically investigated as potential source of the B···Al interaction. The FB···AlF complex, where energetic stabilisation is associated with interaction between the boron and aluminium atoms has been identified. Discovery of this complex stems from our ongoing work on the nature of boron - aluminium covalent bonding [15].

There is currently significant interest in a main-group metal catalysis, expected to reduce the cost, scarcity and toxicity problems associated with some transition metals, present in commonly used industrial catalytic processes. Molecules with B and Al atoms are possible candidates replacing transition metals in such catalytic processes. Detailed knowledge of boron-aluminium interactions (BAl), both covalent and non-covalent, will also play an important role in the design of catalyst replacement candidates such as organoaluminium boryl complexes, metallacarboranes containing aluminium or main group metal analogues of constrained-geometry catalysts.

In this paper, a series of DFT(M062x), MP2 and CCSD(T) calculations have been performed for the FBTF (T= B, Al, Ga, In) and XBAlX (X= Cl, Br, I, At) molecules. Firstly, the optimised structures of the FBTF molecules have been analysed. Secondly, interaction energies and physical nature of weak ditriel B···Al and halogen B···F and Ga···F interactions using Symmetry-Adapted Perturbation Theory (SAPT) [16] are discussed. Occurence of those interactions and their non-covalent nature has been confirmed using the topological analysis of electron density, ρ(r) (AIM) [17,18,19] and electron localisation function, η(r) (ELF) [20]. The changes of the infrared spectra caused by the complex formation are also discussed. Finally the effect of the halogen atom

substitution on the length and population value of the B-Al bond in XBAlX (X= Cl, Br, I, At) set of molecules has been studied. The conclusions close the paper.

II. Computational details

Calculations have been carried out with the Gaussian16 programme, G16, B.01 version, [21]. Molecular structure optimisations have been performed using the CCSD(T)-FC [22,23], MP2(FC) [24] and DFT [25] methods with the exchange-correlation energy functional M062x [26] as implemented in G16. The electrons have been described using the aug-cc-pVTZ [27,28] basis set. For the In, I and At elements the aug-cc-pVTZ-PP pseudopotential and a relevant basis set [29] have been used. The basis sets have been obtained using the Basis Set Exchange software (BSE) [30,31,32]. Stability of the computed wave function has been verified for each optimised system.

The natural population analysis (NPA) [33], as included in G16, has been used for the current densities at the CCSD//CCSD(T) computational levels.

Generation of the molecular orbitals (*wfn*-files) for the topological analysis have been performed in two ways, depending whether the DFT, or CCSD methodology have been chosen for the analysis. For the CCSD(T) optimised structures, the wave function from a single point CCSD/ aug-cc-pVTZ calculation has been used and the approximation proposed by Feixas et al. [34] with the natural orbitals has been adopted. For the molecules containing the In, I or At atoms, when pseudopotential approximation use was essential, the following procedure has been adopted. Firstly the molecular structure has been optimised using aug-cc-pVTZ-PP pseudopotential and relevant basis sets. Then the single point calculations have been carried out using the all-electron triple zeta valence quality plus polarization type basis set („jorge-TZP"), proposed by Martins et al [35] for the In, I and At atoms, while other atoms have been described with the aug-cc-pVTZ basis set. The g-orbitals have been removed from the jorge-TZP basis sets. The all-electron basis set have been obtained using the BSE software.

The SAPT calculations, which utilize the procedure of density fitting (DF) [36], have been performed with the PSI4 program package [37].

Topological analysis of η(r) field has been carried out using the TopMod09 package [38]. The grid step used for the topological analysis was 0.05 bohr. The ELF basins (2D) have been visualized using the VMD [39]. Topological analysis of ρ(r) field has been performed using the AIMall programme [40].

III. Results and discussion

IIIa. Geometrical structures

The structures of the FBTF (T= B, Al, Ga, In) systems, optimised using the DFT(M062x), MP2 and CCSD(T) computational methods are shown in Figure 1. Not all the computational methods used here yielded similar geometry. The result have also been dependent on the triel atom chosen for the analysis.

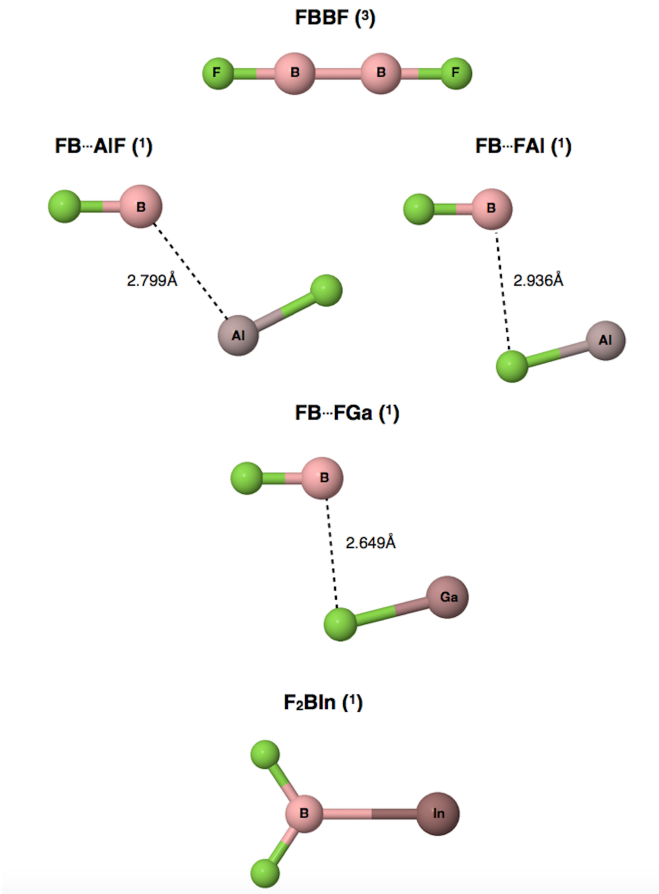

Figure 1. The CCSD(T)/aug-ccpVTZ optimised structures of the FBTF (T= B, Al, Ga, In) molecules.

The FBBF molecule has a linear structure ($D_{\infty h}$), a higher stability is in a triplet state. The molecule has a covalent BB bond, as has been shown previously [41]. The molecule has been studied in fine detail there and will not be discussed here.

For the FBAlF system, the DFT(M062x) and CCSD(T) computational methods yield planar complexes (C_s) in more stable singlet states, showing minima on the potential energy surface (PES). The BF molecule interacts with the AlF molecule in two ways: FB···AlF, and FB···FAl (see Figure 1). From the perspective of atom-atom interactions, the complexes are mainly stabilised by the B···Al ditriel bonding or the B···F triel interaction (FB···FAl).

Optimised values of the boron-triel, r_{opt}(B,T), (T= Al, Ga) and boron-fluorine distances, r_{opt}(B,F), are presented in Table 1. Those large values (> 2.55Å) reveal that both complexes are stabilised by non-covalent molecular interactions. The sum of the van der Waals radii, published by Mantina et al [42] for B (1.92Å) and Al (1.84Å) atoms of 3.76Å, is much larger than the optimised B···Al distance. The CCSD(T) method yields longer r_{opt}(B,T) and r_{opt}(B,F) values than those calculated using the DFT and MP2 methods, thus a proper description of correlation effects play a key role in obtaining correct results. The B···Al separation (2.708Å - DFT, 2.799Å - CCSD(T)) for the FB···AlF complex is much shorter than the B···F distance (2.748 - DFT, 2.936 Å - CCSD(T)) in FB···FAl. This result shows that the metaloid atom (B) - metal atom (Al) interaction is more privileged than the triel B···F bonding. Calculations

using the MP2 method yields only the FB···FAl structure. This suggests that MP2 calculations when studying the B···Al non-covalent ditriel bonding in small systems should be performed with caution.

Table 1. The optimised values of the B···Al (Ga) and B···F distances (in Å), r_{opt}(B,T), in the FB···TF, and FB···FT (T= Al, Ga) complexes. Calculations performed using the DFT(M062x), MP2, CCSD(T) methods with the aug-cc-pVTZ basis set.

Method / System:	FB···AlF	FB···FAl	FB···GaF	FB···FGa
DFT(M062x)	2.708	2.748	2.875	2.568
MP2	-	2.928	-	2.612
CCSD(T)	2.799	2.936	-	2.649

The DFT(M062x) calculations for the FBGaF molecule yield two planar structures (C_s), representing the following minima on the PES: FB···GaF, and FB···FGa. However, only the latter is reproduced with the MP2 and CCSD(T) methods. Thus, the MP2 calculations do not confirm the B···Al and B···Ga ditriel interactions. At the CCSD(T) level the B···F distance of 2.649 Å is clearly shorter than the B···F distance in the FB···FAl complex (2.936 Å). Most probably, a substitution of the Al atom by the less polarisable Ga atom (static dipole polarizability (α_0): Al - 57.8 a.u., Ga - 50 a.u.[43]) results in a less effective B···Ga (dispersion) interaction and leads to the more energetically stable FB···FGa complex. The FB···GaF structure has only been obtained using the simplest DFT(M062x) method, the ditriel B···Ga bonding existence has therefore not been confirmed.

Geometry optimisation for the boron-indium interaction in the FBInF system yields the planar F_2BIn molecule with the C_{2v} point group symmetry. The molecule has the covalent polarised B-In bond and two BF bonds, with predominantly large ionic contribution (see Supplementary material).

In the next sections, we will discuss the FBTF (T= Al, Ga) complexes with the FB···AlF, and FB···FT structures.

IIIb. The interaction energies

Interaction energies, calculated using the DFT(M062x), MP2 and CCSD(T) computational methods, with the basis set superposition error taken into account using the counterpoise technique [44] E_{int}^{CP}, are presented in Table 2. All the methods used show that the complexes stabilised by the ditriel (B···Al, B···Ga) bonding (FB···TF) are less stable than the FB···FT complexes with the B···F triel interaction. Approximately parallel orientation of the dipole moments in the FB···FAl and FB···FGa

structures and a close distance between the positively charged B atom and the negatively charged F atom seem to influence the value of the electrostatic energy contributing to energetic stabilisation.

The ditriel B···Al interaction in the FB···AlF complex is associated with a very small molecular interaction energy (CCSD(T)) of less than 1 kcal/mol (E_{int}^{CP} = -0.90 kcal/mol). Such a small value confirms that the DFT method might be insufficient for the correct description of the ditriel complex properties

Table 2. The values of the interaction energy corrected for the superposition error using the counterpoise correction, E_{int}^{CP}, (in kcal/mol) for the FB···TF, and FB···FT (T= Al, Ga) complexes. Calculations performed using the DFT(M062x), MP2, CCSD(T) methods with the aug-cc-pVTZ basis set.

Method / System:	FB···AlF	FB···FAl	FB···GaF	FB···FGa
DFT(M062x)	-2.71	-3.42	-2.10	-5.02
MP2	-	-2.16	-	-3.07
CCSD(T)	-0.90	-1.98	-	-2.71

In the case of the FB···FAl and FB···FGa complexes, the absolute values of the E_{int}^{CP} decrease in the following order: DFT(M062x) > MP2 > CCSD(T). The studied systems belong to weakly interacting complexes since their E_{int}^{CP} values are smaller than 3 kcal/mol at the CCSD(T) level. A proper description of electron correlation effects is essential for the correct description of their electronic structure.

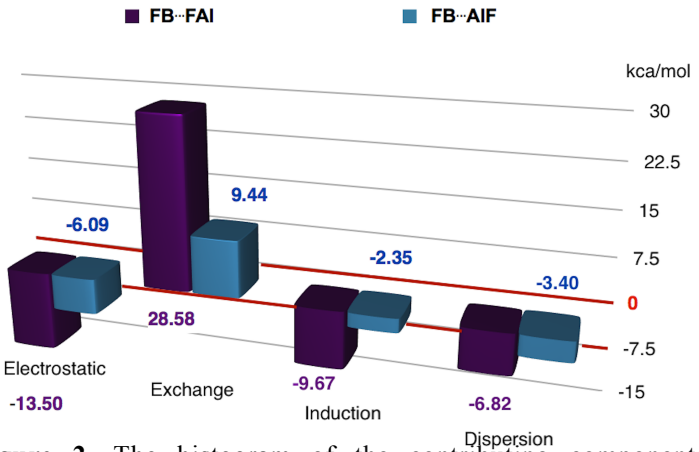

Figure 2. The histogram of the contributing components (electrostatic, exchange, induction, dispersion) to the interaction energy obtained using SAPT (symmetry-adapted perturbation theory) method. The SAPT2+(3) approach has been adopted as described in the PSI4 manual.

The FB···FGa complex, (E_{int}^{CP} = -2.71 kcal/mol), is more stable than the FB···FAl system (E_{int}^{CP} = -1.98 kcal/mol). This result is consistent with a shorter B···F distance in FB···FGa than that observed for the FB···FAl complex.

In order to shed light on the physical nature of interactions stabilising the FB···AlF, FB···FAl, and FB···FGa complexes, the Symmetry Adapted Perturbation Theory (SAPT) has been used (see Computational details). The closed-shell SAPT technique, constrained to second-order expansion of the interaction and fluctuation potentials (monomers), has been applied (E_{SAPT2+}). Additionally, the dispersion

(E_{disp}) and electrostatic (E_{elst}) interaction energies calculated at the third order have been included, $E_{SAPT2+(3)}$ [36].

Graphical comparison of the electrostatic (E_{elst}), exchange (E_{exch}), induction (E_{ind}) and dispersion (E_{disp}) energies (total components) for the FB···AlF and FB···FAl complexes is shown in Figure 2. Absolute values of four energies are clearly larger for the system stabilised with the B···F interaction. Both complexes are not stable at the SCF level, where the exchange energy component dominates over the electrostatic energy. The E_{elst} term yields much effective stabilisation for the FB···FAl complex, due to the total absolute value of 7.41 kcal/mol larger than that calculated for the FB···AlF form. As has been mentioned above, approximately parallel dipole-dipole orientation may have the largest influence on the electrostatic interaction values. The energetic stability is gained at the second order of the interaction potential expansion, when the induction and dispersion energy terms are calculated. For the weaker FB···AlF complex with the ditriel B···Al bonding, the absolute value of E_{disp} is 1.05 kcal/mol larger than E_{ind}. For the more stable FB···FAl complex, the induction energy is dominant with the difference of 2.85 kcal/mol in respect to E_{disp} term.

For the FB···FGa complex, the E_{elec} and E_{exch} components are -11.57 and 18.17 kcal/mol, respectively and the complex is also unstable at the SCF level. Those (absolute) values are smaller than those calculated for the FB···FAl. The stability is gained at the second order of interaction of the potential expansion when the sum of E_{ind} (-4.75 kcal/mol) and E_{disp} (-5.18 kcal/mol), respectively is larger than the sum of the E_{elst} and E_{exch} terms (6.60 kcal/mol). The dispersion energy has larger effect on the total stabilisation than the induction energy has, in contrast to the FB···FAl complexes, where E_{ind} dominates at the second order of the perturbation approach.

IIIc. The infrared frequencies

Formation of the FB···AlF complex is associated with small changes in the harmonic infrared frequencies (IR) for the monomers. The stretching mode of the BF molecule, ν_{str}(B,F) - calculated at 1391.42 cm^{-1} for the complex - moves towards higher frequencies by 10.31 cm^{-1} as compared to the BF monomer (1381.11 cm^{-1}). On the other hand, the ν_{str}(Al,F) mode, calculated at 773.99 cm^{-1} for the complex, is red shifted by 2.29 cm^{-1} in respect to the AlF monomer (776.28 cm^{-1}). Such small changes (absolute values) are consistent with small elongations of the BF (Δr= +0.002Å) and AlF (Δr= +0.002Å) bonds in respective monomers.

The natural population analysis (NPA) shows the $[FB]^{q+}\cdots[AlF]^{q-}$ polarisation formula with the transferred charge of 0.013e. The electronic charge is shifted towards the AlF fragment, formed

by more polarisable Al atom (static dipole polarizability (α_0): B - 20.5 a.u., Al - 57.8 a.u. [43]). In summary, the ditriel B···Al bonding in the FB···AlF complex is a subtle effect of structural and energetic changes manifesting on vibrational excitation of the bonded atoms

For the more stable FB···FAl and FB···FGa complexes, stabilised mainly by the B···F interactions, observed changes in the IR spectra are larger than that found for the complex with ditriel B···Al bonding. For both complexes, the ν_{str}(B,F) mode is blue shifted by 26.38 cm^{-1} and 42.67 cm^{-1}, respectively. On the other hand, the values of the ν_{str}(Al,F) and ν_{str}(Ga,F) modes (627.38 cm^{-1} for the GaF monomer) are moved towards lower frequencies by 24.90 and 45.55 cm^{-1}, respectively. For both structures the relationship with the the monomer's bond changes is clearer in this case than for weaker the FB···AlF complex. The BF molecule is shortened (Δr= -0.004Å, -0.006Å), while the AlF and GaF molecules are elongated (Δr= +0.012Å, +0.028Å) as a result of existing intramolecular forces.

The NPA shows the $[FB]^{q+}\cdots[FAl]^{q-}$ and $[FB]^{q+}\cdots[FGa]^{q-}$ polarisation of the complexes with electronic charge flowing from the BF to the AlF and GaF molecules. The transferred charge, Δq, is 0.018e and 0.043e, respectively. These values are larger than those obtained for the FB···AlF complex and they correspond to the larger interaction energy E_{int}^{CP} related to the systems stabilised by the B···F interaction and parallel orientations of the molecular dipole moments.

IIId. Topological analysis of ρ(r) field

In order to identify atomic interactions responsible for the energetic stabilisation of the FB···AlF, FB···FAl, and FB···FGa complexes, the topological analysis of electron density, ρ(r), field has been performed as proposed by Bader [17-19]. The atomic basins (quantum atoms), attractors, bond critical points (BCPs) of ρ(r), and the contours of the Laplacian of ρ(r), $\nabla^2\rho(r)$, for the FB···AlF complex are presented in Figure 3a. Similar plots are shown in Figure 3b for the FB···FAl complex. A very similar topology of ρ(r) and $\nabla^2\rho(r)$ has been obtained for the FB···GaF and FB···FGa complexes, therefore they will not be discussed here. Numerical values calculated for the BCPs and quantum atoms are collected in Table 3. The results for the FB···FGa complex will not be discussed in details due to their similarity to the results obtained for the FB···FAl complex

The net atomic charges calculated as an average number of electrons in the quantum atoms (see Figure 3) clearly indicate that the complexes consist of positively ($B^{\delta+}$, $Al^{\delta+}$) and negatively charged ($F^{\delta-}$) ions with a charge about 0.9e. It is worth noting that the aluminium atom bears larger charge (+0.986e, +0.952e) than the boron atom (+0.866e, +0.915e). The picture of the complexes

formed by ions is consistent with large contributions of the electrostatic components to the total interaction energies.

The electronic structure of the FB···AlF complex is characterised by three bond critical points (BCPs), (3,-1), associated with the FB, AlF and B···Al interactions. Thus, the ditriel B···Al bonding has been confirmed. The bonding path joining the nuclei attractors (3,-3) CP, localised at the B and Al nuclei can be seen in Figure 3a. For the FB···FAl complex the B···F interaction has also been confirmed by the localisation of BCP.

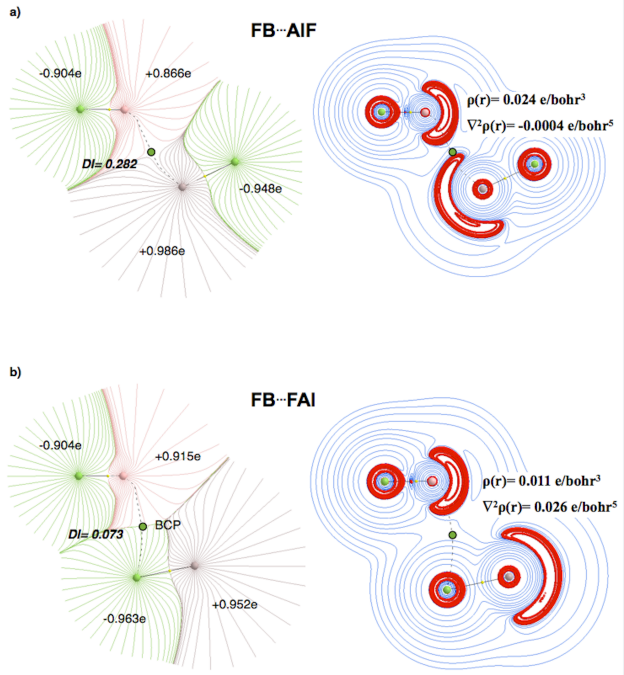

Figure 3. 2D plots of the atomic basins (quantum atoms) and Laplacian of ρ(r) (red - negative) with marked values of the net atomic charges, the delocalisation index (DI), ρ(r) for BCP, and $\nabla^2\rho(r)$ for BCP for: a) the FB···AlF complex with the ditriel bonding, b) FB···FAl complex with the halogen bonding.

Analysis of the ρ(r) for the BCPs shows small differences in values. For the shorter B···Al interaction in the FB···FAl complex the value of ρ(r) is about two times (2.18) larger than for the longer B···F interaction. It is bound to be associated with a larger polarisability of the Al atom.

Analysis of the $\nabla^2\rho(r)$ contours confirms non-covalent nature of the ditriel B···Al bonding interaction. The positive values of $\nabla^2\rho(r)$ between atomic nuclei are observed (BCP), thus any signs of the shared-electron bonding is missing. It is worth emphasizing the difference between the maps of $\nabla^2\rho(r)$ for the B···Al and B···F bondings. For the B···Al interaction, two separate areas with negative values in the vicinity of the B and Al atoms are positioned opposite each other, while for the B···F interaction the area with negative values (B atom) is in 'contact' with the area with positive values around the F atom.

For the B···F interaction the BCP is localised within the region with positive values (0.026 e/bohr^5) of $\nabla^2\rho(r)$. Thus, the interaction belongs to the closed-shell type. For the ditriel B···Al bonding the value of $\nabla^2\rho(r)$ for BCP is very small and negative ($-4\cdot10^{-4}$ e/bohr^5), due to the BCP location at the edge of the negative area of $\nabla^2\rho(r)$ in the vicinity of the Al atom (see Figure 3a). The larger absolute value of $\nabla^2\rho(r)$ for the B···F bonding coincides with a larger strength of the B···F interaction, indicated by the larger value of E_{int}^{CP}. Due to a very small value of the $\nabla^2\rho(r)$ value for BCP, it is

difficult to conclude a partial covalent nature of the B···Al bonding, however it seems that the nature of the B···Al and B···F interactions is not the same.

Table 3. The numerical parameters for the bond critical point of the ditriel interaction in the the FB···TF, and FB···FT (T= Al, Ga) complexes. Calculations performed using the DFT(M062x), MP2, CCSD(T) methods with the aug-cc-pVTZ basis set.

Method / System	**FB···AlF**					**FB···FAl**				
Param:	**ρ(r)**	**$\nabla^2\rho(r)$**	**H(r)**	**ε(r)**	**DI**	**ρ(r)**	**$\nabla^2\rho(r)$**	**H(r)**	**ε(r)**	**DI**
DFT(M062x)	0.027	0.003	-0.006	0.094	0.418	0.015	0.035	-0.0001	1.254	0.112
MP2	-	-	-	-		0.011	0.026	-0.0001	0.835	0.083
CCSD(T)	0.024	0.0004	-0.005	0.128	0.282	0.011	0.026	-0.0002	0.553	0.073
Method / System	**FB···GaF**					**FB···FGa** [1)]				
DFT(M062x)	0.022	0.016	-0.003	0.006	0.325	0.019	0.053	-0.0003	0.662	0.135
MP2	-	-	-	-	-	0.020	0.046	-0.0007	1.673	0.180
CCSD(T)	-	-	-	-	-	0.015	0.038	-0.0001	0.998	0.088

[1)] the topological analysis of ρ(r), carried out using MP2 method, also shows the BCP for the B···Ga interaction with: ρ(r)= 0.0190 e/bohr^3, $\nabla^2\rho(r)$= -0.0311 e/bohr^5, H(r)= -0.002 hartree/bohr^3, ε(r)= 1.316, DI= 0.180

ρ(r) - the electron density for the bond critical point (BCP), $\nabla^2\rho(r)$ - Laplacian of the electron density for BCP, H(r) - the total energy density for BCP, ε(r) - the ellipticity for BCP, DI - delocalisation index for the B and Al quantum atoms and B and F quantum atoms

The exchange of electron pairs between B and Al quantum atoms, as measured by the delocalisation index (DI), is very small (< 0.3e), about 4 times smaller for the B···F interaction (0.073). This result clearly shows that both B···Al and B···F bonds do not belong to a shared electron type of interactions.

In summary the B···F interaction belongs to a class of very weak, non-covalent interactions. The non-covalent ditriel B···Al bonding exhibits distinctive features as compared to the B···F bonding.

IIIe. Topological analysis of electron localisation function (ELF) field

The topological analysis of the Electron Localisation Function (ELF), η(r) [45] developed by Silvi et al [20,46,47,48,49], enables an additional analysis for both covalent and non-covalent interactions. The attractors of η(r) field correspond to atomic shells, covalent bonds and lone pairs (non-bonding electron density) representing a classical representation of the electronic structure in the Lewis formula.

The FBBF (triplet state) molecule has been investigated previously [41]. The covalent BB bond is described by V(B,B) disynaptic basin with 3.92e at the DFT(M062x) computational level. Thus, the interaction can be approximately classified as the double B=B bond. Two BF bonds, described by the V(B,F) disynaptic basins, have basin populations, $\bar{N}$, of 1.65e. Those bonds should be characterised as covalent-polarised and described by two resonance forms, B-F (dominant) and $B^{+}F^{-}$.

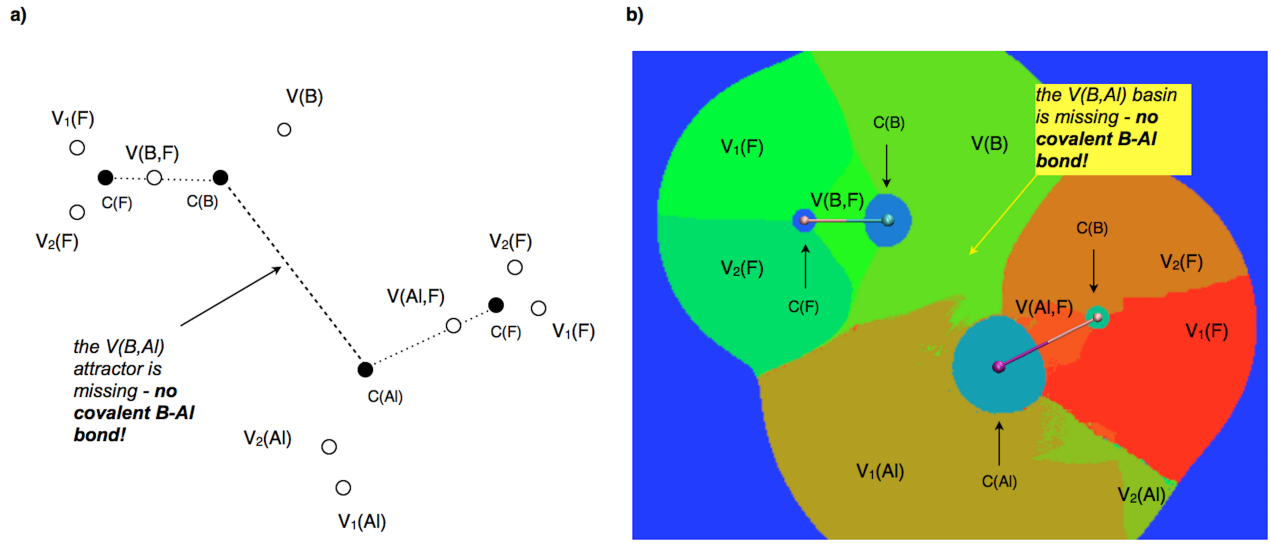

Figure 4. a) the core and valence attractors for the FB···AlF complex, b) partition of the molecular space of the FB···AlF complex into attractor's basins. The presented slice has been chosen slightly above the symmetry plane, therefore the points associated with the V_2(Al) attractor (basins) are hardly visible. Calculations performed at the CCSD/aug-cc-pVTZ//CCSD(T)/aug-cc-pVTZ computational level.

In the case of the FB···AlF complex (CCSD//CCSD(T)), 13 core and valence attractors have been localised in the η(r) field as presented in Figure 4 and the numerical data are collected in Table 5. No valence attractor of ELF is observed in the area between the B and Al nuclei, where B···Al bonding is expected. The ditriel interaction has therefore a non-covalent character. The valence electron density (the B···Al region) is characterised by three non-bonding disynaptic attractors: V(B) and V_1(Al), V_2(Al), because the symmetry of the non-bonding electron density of Al is described by two attractors, V_1(Al), V_2(Al), found below and above the molecular plane. Only one monosynaptic attractor, V(B), is found for the boron atom. All three attractors are localised in the positions suggesting the avoidance of the the B and Al atoms' lone pairs (Pauli repulsion). This seems to be an effect of mutual attraction/repulsion of both subunits as characterised by the SAPT analysis. The basin populations for V(B) and V_1(Al), V_2(Al) of 2.11e and 0.95, 0.96e (total 1.91e) confirm a classical concept of single lone pairs in the vicinity of the C(B) and C(Al) cores. Thus, the bonding in the FB···AlF complex can be represented by the Lewis structure shown in Scheme 1. T h r e e

formal lone pairs at each F atom are reflected by two pairs of basins, $V_1(F)$, $V_2(F)$, localised in the molecular plane due to the planar symmetry. The total basin population of 6.0e (3.06 and 2.94e) for the F atom of BF supports perfectly the concept of three lone pairs as can be seen in Scheme 1. For the F atom from the AlF molecule with two $V_1(F)$, $V_2(F)$ basins, characterised by population of 5.00e and 1.84e, respectively (6.84e in total), three lone pairs with additional electron can be expected. It is worth noting the difference in population of non-bonding basins of F in BF with 6.0e, and for F in AlF with 6.84e. It reflects the fact, that Al atom is much electropositive than the B atom and approximately one electron is donated to the valence space of F. This result is not surprising due to high electropositivity, typical for metals. Topological analysis of η(r) field shows that the AlF bond character is essentially less covalent than that of the BF bond.

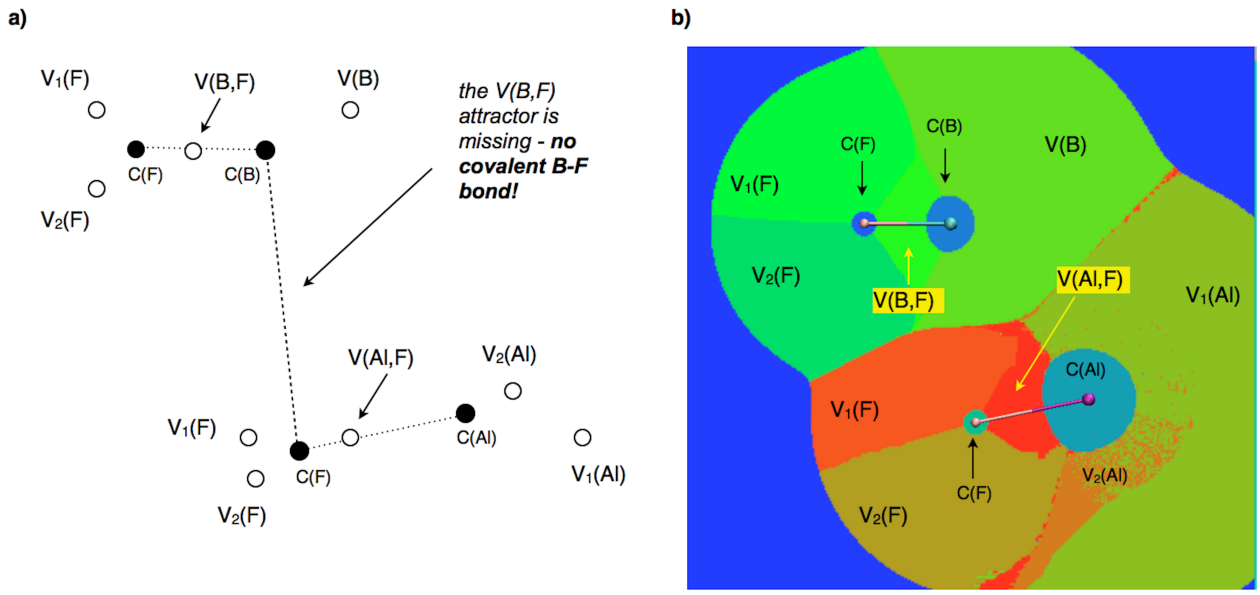

Figure 5. a) the core and valence attractors for the FB···FAl complex, b) partition of the molecular space of the FB···FAl complex into attractor's basins. The presented slice has been chosen slightly above the symmetry plane, therefore the points associated with the $V_2(Al)$ attractor (basins) are hardly visible. Calculations performed at the CCSD/aug-cc-pVTZ//CCSD(T)/aug-cc-pVTZ computational level.

A further study of formally single BF and AlF bonds is essential in order to fully characterise the electronic structure of the FB···AlF complex. The bonds are characterised by the disynaptic basins V(B,F) and V(Al,F), which suggests their partially covalent nature. Analysis of Figure 4b confirms a disynaptic character of the basins, due to a common surface between the C(B), C(F) core basins in BF and C(Al), C(F) core basins in AlF. According to Silvi et al [48], the disynaptic type of basins is confirmed by two-center character of the B-F and Al-F bonds.

A classical concept of the ionic and covalent bonds can be verified by analysing an amount of electron density in the bonding basin. This way, topological analysis of ELF provides a chemical

interpretation. Basin population of V(B,F) of 1.73e, smaller than 2e expected for the 2c-2e covalent bond, suggests partially covalent bonding with ionic contribution. The bonding can be described using two resonance structures: the covalent B-F and ionic B^+F^-.

A lack of typical covalent character is found for the AlF bond, with a small population of 1.02 e for the V(Al,F) basin. This result explains a large population of 6.84e found for $V_1(F)$, $V_2(F)$ basins - one electron is transferred from the bonding region to the non-bonding region of F atom. The small value of the $\bar{N}$ for V(Al,F) confirms that the bond is not typically covalent. Basin populations of 1e and less are treated as a possible indication of the charge-shift bonding [50]. The

Table 4. Basin populations ($\bar{N}$) and atomic contributions to the localisation basins (Ω_i,) for the attractors localised in the field of η(r) function for the FB···AlF and FB···FAl complexes. Calculations performed at the CCSD/aug-cc-pVTZ// CCSD(T)/aug-cc-pVTZ computational level. The basin population for the C(F) basin is the same for both molecules.

Basin Ω_i,	**$\bar{N}$ [e]**	**atomic contribution [e]**	**$\bar{N}$ [e]**	**atomic contribution [e]**
	FB···AlF		**FB···FAl**	
	core basins			
C(B)	2.05	2.05 (B)	2.05	2.05 (B)
C(F)	2.14	2.14 (F)	2.15	2.15 (F)
C(Al)	10.04	10.04 (Al)	10.04	10.04 (Al)
	nonbonding basins			
V(B)	2.11	0.10 (F), 1.99 (B)	2.07	0.10 (F), 1.96 (B)
$V_1(F)$	2.94	2.94 (F)	2.22	2.22 (F)
$V_2(F)$	3.06	3.06 (F)	3.74	3.74 (F)
$V_1(Al)$	0.95	0.92 (Al)	0.97	0.95 (Al), 0.02 (F)
$V_2(Al)$	0.96	0.93 (Al)	0.98	0.96 (Al), 0.02 (F)
$V_1(F)_{AlF}$	1.84	1.83 (F)	3.78	3.76 (F)
$V_2(F)_{AlF}$	5.00	4.95 (F)	2.74	2.73 (F)
	bonding basins			
V(B,F)	1.73	1.65 (F), 0.08 (B)	1.75	1.68 (F), 0.08 (B)
V(Al,F)	1.02	0.99 (F), 0.03 (Al)	1.33	1.25 (F), 0.05 (Al)

standard deviation for V(Al,F) of 0.82 shows that electron density of the basin is highly delocalised and the Al^+F^- ionic structure dominates in the resonance equilibrium of the Al^+F^-, Al·F forms.

Finally, the concept of A and B atomic contribution to a localisation basin V(A,B), proposed by Raub and Jansen [51], has been applied. The polarity index, p_{AB}, has a value between 0 and 1 with the former indicating homopolar bonds and the latter for idealised ionic bonds. Interestingly, the V(B,F) basin consists of 1.65e (95%) from the F atom and only 0.08e (5%) from the B atom (p_{FB}=0.91). Thus, the bond actually is formed mainly by fluorine and the two-center, partial covalent BF bond is highly polarised. In the case of the AlF bond, the V(Al,F) basin with 1.33e consists of 1.25e (94%) from the F atom and 0.05e (4%) from the Al atom (p_{FAl}=0.92). Similar interpretation to the above can be applied here. The delocalised electron density 'contained' in the V(Al,F) basin comes mainly from the fluorine valence shell. The electron cloud of two-center BAl bond is highly polarised towards the F atom. Other values of the atomic contributions are presented in Table 5.

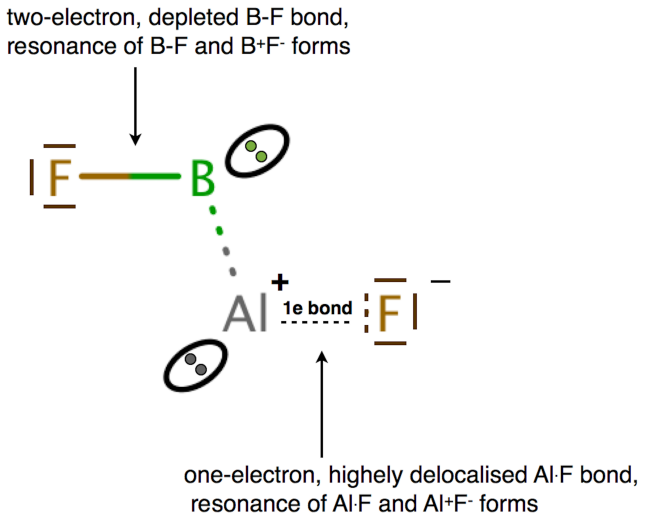

Scheme 1. The Lewis formula for the FB···FAl complex obtained using the results of topological analysis of ELF. The dashed vertical line and three solid vertical lines in the vicinity of the F atom in the AlF molecule are related to the total basin population of the valence electrons (6.84e).

In summary, using the Lewis classical language, we believe that the bonding representation in the FB···AlF complex is as presented in Scheme 1, represented by both covalent B-F and ionic B^+F^- resonance structures for the BF bond, highely delocalised one-electron Al·F bond and Al^-F^+ Al^+F- ionic forms for the AlF. The ditriel B···Al bonding is actually an interaction between two positively charged atoms, while the B···F triel bonding is an interaction between positively and negatively charged atoms.

IIIf. Influence of halogen atoms on the nature of the BAl bonding.

In order to check whether the nature of the ditriel B···Al bonding depends on the halogen type, a set of the XBAlX (X= Cl, Br, I, At) molecules have been studied using the DFT(M062x) method with the aug-cc-pVTZ (Cl, Br) and aug-cc-pVTZ-PP (I, At) basis sets. The optimised

geometries for all the structures in their singlet states are similar (see Figure S1) regardless of the halogen atom (X= F-At). The optimised lengths of the B-Al bond, r_{opt}(B,Al), are shown in Table 5.

Table 5. The optimised distances of the boron-aluminium bond, r_{opt}(B,Al), and the population values, $\bar{N}$, for the V(B,Al), V(B,X) and V(Al,X) basins localised in the XBAlX (X= Cl, Br, I, At) molecules. Calculations performed at the DFT(M062x)/aug-cc-pVTZ (Cl, Br) and DFT(M062x)/ aug-cc-pVTZ-PP (I, At) computational levels.

Atom / Param.	r_{opt}(B,Al) [Å]	$\bar{N}$ [V(B,Al)] [e]	$\bar{N}$ [V(B,X)] [e]	$\bar{N}$ [V(Al,X)] [e]
Cl	2.318	2.43	1.76	1.41
Br	2.277	2.47	1.72	1.45
I	2.231	2.52	1.74	1.57
At	2.240	2.51	1.68	1.45

Substituting the F atom by a heavier halogen results in shortening of the BAl bond from 2.708Å (F) to much shorter bonds between 2.240Å (At) - 2.318Å (Cl). For such short atomic interactions, a covalent character with shared electron density in the bond can be expected. The results clearly show that the ditriel B···Al bonding is an unique feature of the interaction between the $B^{\delta+}$ and $Al^{\delta+}$ charged atoms. As expected, a covalent character of the B-Al bond has been confirmed by the topological analysis of ELF, showing the disynaptic bonding attractor V(B,Al) for all the XBAlX molecules. The basin populations range between 2.43 (Cl) and 2.52e (I) and are much larger than 2e expected for a single bond. The boron-aluminium bond in the XBAlX (X= Cl, Br, I, At) systems has an interim character, between a single B-Al and a double B=Al bond, when the Lewis representation is used, but with a significant dominance of a single bond. Interestingly, the relationship between the B-Al bond length and the V(B,Al) basin population is almost linear as presented in Figure 6.

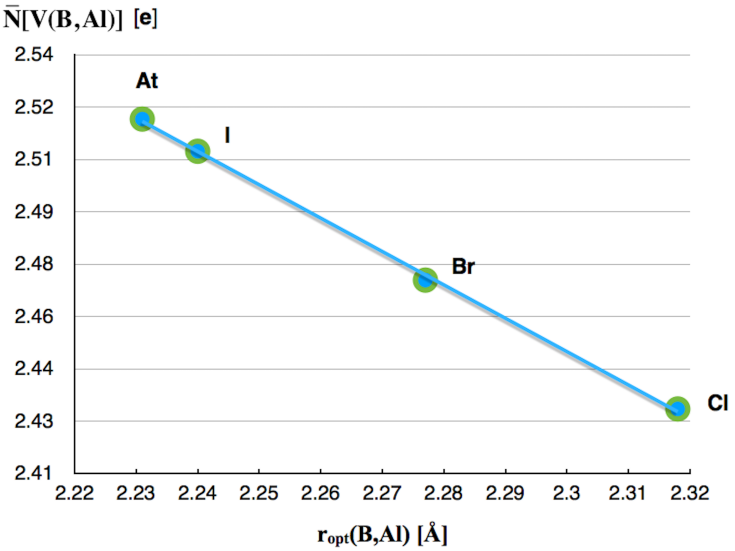

Figure 6. The relationship between the population, $\bar{N}$ [e] of the B-Al bond, represented by the V(B,Al) bonding disynaptic basin, and the optimised length, r_{opt}(B,Al) [Å] for the XBAlX (X= Cl, Br, I, At) molecules. Calculations performed at the DFT(M062x)/aug-cc-pVTZ (Cl, Br) and DFT(M062x)/ aug-cc-pVTZ-PP (I, At) computational levels. Dependence between the values of $\bar{N}$ and r_{opt}(B,Al) has been investigated using linear regression (r^2= 0.999).

For the BX and AlX bonds, topological analysis of ELF also shows a two-center and partially covalent character of the bonding. The V(B,X) and V(Al,X) disynaptic attractor and

basins are localised in the regions between the boron and halogen and between the aluminium and halogen cores. Corresponding values of the $\bar{N}$ basin population are presented in Table 5. The values of $\bar{N}$ are smaller than 2e. The BX and AlX bonds show much smaller covalent character than the BAl bond based on the value expected for the single bond. This can be explained by a partially ionic character of the bonding. Therefore, the equilibrium of the B-X, $B^{+}X^{-}$ and Al-X, $Al^{+}X^{-}$ resonance structures should be considered. The basin populations of V(Al,X) are smaller ($\Delta\bar{N}$ = 0.17-0.35e) than these calculated for the V(B,X) basins, therefore a contribution of ionic forms is larger for the AlX bonding.

IV. Conclusions

Theoretical studies performed for the FBTF (T= B, Al, Ga, In) and XBAlX (X= Cl, Br, I, At) molecules show a variety of structural and binding motifs, including covalent BB, BIn and BAl bonds in the FBBF, F_2BIn and XBAlX molecules. The FB···AlF and FB···GaF molecular complexes exhibit structures stabilised with the B···Al and B···F non-covalent interactions.

The ditriel B···Al bonding has been identified only in the $F^{\delta-}B^{\delta+}\cdots Al^{\delta+}F^{\delta-}$ molecular complex, which has a clearly ionic structure of the components (AIM: $\delta\approx$ 0.9e). The presence of the interaction stabilising the molecule has been confirmed by a bond critical point localised on the gradient path joining B and Al nuclei attractors in the field of ρ(r). Topological analysis of ELF shows that the ditriel B···Al bonding has a non-covalent character, due to absence of the V(B,Al) disynaptic attractor. The bond is very weak due to very small values of ρ(r), $\nabla^2\rho(r)$ and H(r) numerical parameters for BCP. A very weak character of the bonding is also confirmed by a very small value of the interaction energy, E_{int}^{CP} (less than 1 kcal/mol) at the CCSD(T) level.

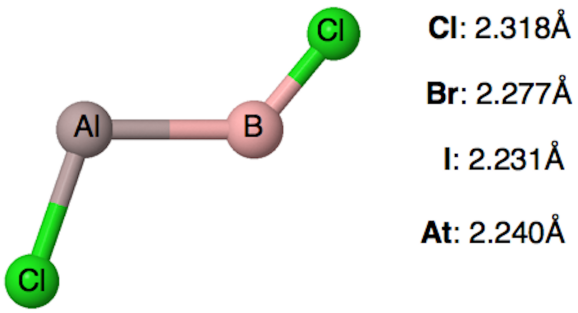

Figure S1. The geometrical structure of the ClBAlCl molecule optimised at the DFT(UM062x)/aug-cc-PVTZ computational level. The BrBAlBr molecule has been optimised at the DFT(UM062x)/aug-cc-PVTZ computational level and the XBAlX (X= I, At) molecules at the DFT(UM062x)/aug-cc-pVTZ-PP computational level. The optimised structures of all molecules are very similar.

The formation of the ditriel B···Al bonding is an unique feature, emerging from stabilisation of the $B^{\delta+}Al^{\delta+}$ fragment by two F anions.

The ditriel bond has neither been found in analogous compounds FBTF (T= B, Ga, In), nor in in the XBAlX (X= Cl, Br, I, At) molecules, where only a single B-Al bond has been only observed.

From the reductionist point of view („Atoms in molecule" theory) the $F^{\delta-}B^{\delta+}\cdots Al^{\delta+}F^{\delta-}$ molecular complex is stabilised by the ditriel B···Al bonding as well as by the FB and AlF atomic interactions. On the other hand, considering the molecular complex as a whole in terms of SAPT methodology, rather than merely the „sum" of its atoms, leads to the conclusion that stability results from the dispersion and induction forces present between the $F^{\delta-}B^{\delta+}$ and $Al^{\delta+}F^{\delta-}$ subunits.

V. Acknowledgments

The authors are grateful to the Wroclaw Centre for Networking and Supercomputing for generous allocation of computer time.

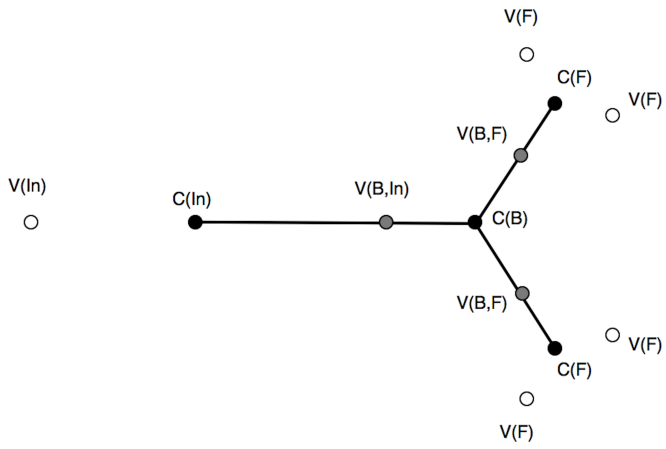

Figure S2. The core and valence attractors for the FBInF molecule.

VI. Conflicts of interest

The authors declare no conflict of interest with regard to the publication of this article.

Supplementary material:

The analysis of bonding in FBInF

The analysis of bonding shows twelve core and valence attractors. The core and valence attractors are shown in Figure S2. The core basins characterise: C(F) - fluorine core, C(B) - boron core, and C(In) - indium core with 2.14e, 2.06e and 45.76e ([Kr] $4d^{10}$). Three bonding disynaptic attractors, V(B,F), V(B,F), V(B,In), are localised in the valence space, characterising two-centre covalent-polarised bonds B-F, B-F and B-In. Such bonds classically are described as formed by 2e, but topological analysis of ELF shows the basin populations of 1.36e, 1.36e and 2.15e. The B-In bond can be characterised as a single bond based on the Lewis formula. On the other hand two BF bonds exhibit highly electron-deficient bonds and electronic structure, which can be represented by the B-F, B^+F^- resonance formulas. Some amount of electron density is divided among the non-bonding disynaptic basins and this can be associated with a formal concept of lone pairs in Lewis formula. Such lone pairs on the F atom are represented by two basins V(F), V(F) with 3.20, 3.21e yielding 6.41e in total, which

roughly corresponds to three formal lone pairs. Additionally, the monosynaptic attractor V(In) is found in the vicinity of the C(In) core with localisation basin population of 2.16e. Thus, one formal lone pair on In atom has been confirmed.

Atomic contributions to the V(B,In) basin of 0.62e (In) and 1.42e (B) show that the B-In bond is polarised towards the boron atom with the polarity index, p_{BIn}, of 0.39. Interestingly, the B atom donates a large amount of density, despite possessing empty p orbitals. A completely different picture has been obtained for two BF bonds. They are formed mainly by electron density from the F atom with 1.27e with a very small contribution of 0.10e from the B atom. Polarisation of the bond is very large, due to the polarity index, p_{FB}, of 0.85.

VII. References

[1] K. Liu, Y. Kang, Z. Wang and X. Zhang, *Adv. Mater.,* 2013, **25**, 5530-5548. https://doi.org/10.1002/adma201302015

[2] D. Braga and F. Grepioni, *Acc. Chem. Res.,* 2000, **33**, 601–608. https://doi.org/10.1021/ar990143u

[3] S. E. Wheeler, T. J. Seguin, Y. Guan and A. C. Doney, *Acc. Chem. Res.,* 2016, **49**, 1061–1069. https://doi.org/10.1021/acs.accounts.6b00096

[4] J−P. Sauvage, P. Gaspard (Eds), From Non-Covalent Assemblies to Molecular Machines, Wiley−VCH, Weinheim, 2011.

[5] M. Debnath, S. Chakraborty, Y. P. Kumar, R. Chaudhuri, B. Jana and J. Dash, *Nat. Commun.,* 2020, **11**, 469. https://doi.org/10.1038/s41467-019-13834-7

[6] I. Alkorta, J. Elguero, A. Frontera and P. J. Lusby, *Crystals,* 2020, **10,** 180. https://doi.org/10.3390/cryst10030180

[7] E. C. Escudero-Adán, A. Bauzá, C. Lecomte, A. Fronterab and P. Ballestera, *Phys. Chem. Chem. Phys*., 2018, **20**, 24192-24200.

[8]S. J. Grabowski, *Coord. Chem. Rev.,* 2020, **407** 213171. https://doi.org/10.1016/j.ccr.2019.213171.

[9] M. D. Esrafili and P. Mousavian, *Mol. Phys.,* 2018, **116**, 388-398. https://doi.org/10.1080/00268976.2017.1393118

[10] S. J. Grabowski, *Molecules,* 2015, 20, 11297-11316. https://doi.org/10.3390/molecules200611297/

[11] S. J. Grabowski, *Molecules,* 2020, **25**, 2703. https://doi.org/10.3390/molecules25112703

[12] J. Zhang, Z. Wang, S. Liu, J. Cheng, W. Li and Q. Li, *Appl. Organomet. Chem.,* 2019; **33**, e4806. https://doi.org/10.1002/aoc.4806

[13] S. J. Grabowski, *Crystals*, 2019, **9**, 503. https://doi.org/10.3390/cryst9100503

[14] P. Politzer and J.S. Murray, *J. Comput. Chem.,* 2018, **39**, 464–471. https://doi.org/10.1002/jcc.24891

[15] S. Berski and A. J. Gordon, „The covalent and non-covalent boron-aluminum interactions from perspective of the topological study of ELF function" in preparation

[16] B. Jeziorski, R. Moszynski and K. Szalewicz, *Chem. Rev.,* 1994, 94, 1887–1930. https://doi.org/10.1021/cr00031a008

[17] R. F. W. Bader, Atoms in Molecules: A Quantum Theory, Clarendon Press, Oxford, 1990.

[18] R. F. W. Bader, *Acc. Chem. Res.,* 1985, **18**, 9–15. https://doi.org/10.1021/ar00109a003

[19] R. F. W. Bader, *Chem. Rev.,* 1991, **91**, 893–928. https://doi.org/10.1021/cr00005a013

[20] B. Silvi, I. Fourré and M. Alikhani, *Monatsh. Chem.,* 2005, **136**, 855–879. https://doi.org/10.1007/s00706-005-0297-8

[21] Gaussian 16, Revision B.01, M. J. Frisch, G. W. Trucks, H. B. Schlegel, G. E. Scuseria, M. A. Robb, J. R. Cheeseman, G. Scalmani, V. Barone, G. A. Petersson, H. Nakatsuji, X. Li, M. Caricato, A. V. Marenich, J. Bloino, B. G. Janesko, R. Gomperts, B. Mennucci, H. P. Hratchian, J. V. Ortiz, A. F. Izmaylov, J. L. Sonnenberg, D. Williams-Young, F. Ding, F. Lipparini, F. Egidi, J. Goings, B. Peng, A. Petrone, T. Henderson, D. Ranasinghe, V. G. Zakrzewski, J. Gao, N. Rega, G. Zheng, W. Liang, M. Hada, M. Ehara, K. Toyota, R. Fukuda, J. Hasegawa, M. Ishida, T. Nakajima, Y. Honda, O. Kitao, H. Nakai, T. Vreven, K. Throssell, J. A. Montgomery, Jr., J. E. Peralta, F. Ogliaro, M. J. Bearpark, J. J. Heyd, E. N. Brothers, K. N. Kudin, V. N. Staroverov, T. A. Keith, R. Kobayashi, J. Normand, K. Raghavachari, A. P. Rendell, J. C. Burant, S. S. Iyengar, J. Tomasi, M. Cossi, J. M. Millam, M. Klene, C. Adamo, R. Cammi, J. W. Ochterski, R. L. Martin, K. Morokuma, O. Farkas, J. B. Foresman, and D. J. Fox, Gaussian, Inc., Wallingford CT, 2016.

[22] R.J. Bartlett and G.D. Purvis III, *Int. J. Quantum Chem.,* 1978, **14**, 561-581. https://doi.org/10.1002/qua.560140504

[23] G.D. Purvis III and R.J. Bartlett, *J. Chem. Phys.,* 1982, **76**, 1910-1918. https://doi.org/10.1063/1.443164

[24] Chr. Møller and M. S. Plesset, *Phys. Rev.,* 1934, **46**, 618–622. https://doi.org/10.1103/PhysRev.46.618

[25] R.G. Parr and W.Yang, Density-Functional Theory of Atoms and Molecules, Oxford University Press, New York, 1989.

[26] Y. Zhao and D.G. Truhlar, *Theor Chem Acc.,* 2006, 120, 215–241. https://doi.org/10.1007/s00214-007-0310-x

[27] T.H. Dunning, *J. Chem. Phys.* 1989, **90**, 1007–1023. https://doi.org/10.1063/1.456153

[28] R.A. Kendall, T.H. Dunning Jr. and R.J. Harrison, *J. Chem. Phys.,* 1992, **96**, 6796-6806. https://doi.org/10.1063/1.462569

[29] K. A. Peterson, D. Figgen, E. Goll, H. Stoll and M. Dolg, *J. Chem. Phys.,* 2003, **119**, 11113-11123. https://doi.org/10.1063/1.1622924

[30] B. P. Pritchard, D. Altarawy, B. Didier, T. D. Gibson and T. L. Windus. *J. Chem. Inf. Model.,* 2019, **59**, 4814-4820, doi:10.1021/acs.jcim.9b00725.

[31] D. Feller, *J. Comp. Chem.,* 1996, **17**, 1571-1586. https://doi.org/10.1002/(SICI)1096-987X(199610)17:13<1571::AID-JCC9>3.0.CO;2-P

[32] K. L. Schuchardt, B. T. Didier, T. Elsethagen, L. Sun, V. Gurumoorthi, J. Chase, J. Li and T.L. Windus *J. Chem. Inf. Model.,* 2007, **47**, 1045-1052. doi:10.1021/ci600510j.

[33] A. E. Reed, R. B. Weinstock and F. Weinhold, *J. Chem. Phys.* 1985, **83**, 735-746 . https://doi.org/10.1063/1.449486

[34] F. Feixas, E. Matito, M. Duran, M. Solá and B. Silvi, *J. Chem. Theory Comput.,* 2010, **6,** 2736-2742. https://doi.org/10.1021/ct2001123

[35] L. S. C. Martins, F. E. Jorge and S. F. Machado *Mol. Phys.,* 2015, **113**, 3578-3586 https://doi.org/10.1080/00268976.2015.1040095

[36] T. M. Parker, L. A. Burns, R. M. Parrish, A. G. Ryno and C. D. Sherrill, *J. Chem. Phys.,* 2014, **140,** 094106. https://doi.org/10.1063/1.4867135

[37] Psi4 1.1: An Open-Source Electronic Structure Program Emphasizing Automation, Advanced Libraries, and Interoperability, R. M. Parrish, L. A. Burns, D. G. A. Smith, A. C. Simmonett, A. E. DePrince III, E. G. Hohenstein, U. Bozkaya, A. Yu. Sokolov, R. Di Remigio, R. M. Richard, J. F. Gonthier, A. M. James, H. R. McAlexander, A. Kumar, M. Saitow, X. Wang, B. P. Pritchard, P. Verma, H. F. Schaefer III, K. Patkowski, R. A. King, E. F. Valeev, F. A. Evangelista, J. M. Turney, T. D. Crawford, and C. D. Sherrill, J. Chem. Theory Comput., 13 (2017) 3185–3197. https://doi.org/10.1021/acs.jctc.7b00174

[38] S. Noury, X. Krokidis, F. Fuster and B. Silvi, *Comp & Chem.* 1999, **23**, 597-604. https://doi.org/10.1016/S0097-8485(99)00039-X

[39] W. Humphrey, A. Dalke and K. Schulten, *J. Mol. Graphics,* 1996, **14**, 33–38. https://doi.org/10.1016/0263-7855(96)00018-5

[40] AIMAll (Version 17.01.25) Todd A. Keith, TK Gristmill Software, Overland Park KS, USA, 2017 (aim.tkgristmill.com)

[41] G. Mierzwa, A. J. Gordon and S. Berski *J. Mol. Struct.* 2020, 1221, 128530. https://doi.org/10.1016/j.molstruc.2020.128530/

[42] M. Mantina, A. C. Chamberlin, R. Valero, Chr. J. Cramer and D. G. Truhlar, *J. Phys. Chem. A* 2009, **113**, 5806–5812. https://doi.org/10.1021/jp8111556

[43] P. Schwerdtfeger and J. K. Nagle, *Mol. Phys.,* 2019, **117**, 1200-1225. https://doi.org/10.1080/00268976.2018.1535143

[44] S. F. Boys and F. Bernardi, *Mol. Phys.,* 1970, **19**, 553-566. https://doi.org/10.1080/00268977000101561

[45] A. D. Becke and K. E. Edgecombe, *J. Chem. Phys.,* 1990, **92**, 5397. https://doi.org/10.1063/1.458517

[46] B. Silvi, and A. Savin, *Nature,* 1994, **371**, 683–686. https://doi.org/10.1038/371683a0

[47] A. Savin, B. Silvi and F. Colonna, *Can. J. Chem.,* 1996, **74**, 1088 - 1096. https://doi.org/10.1139/v96-122

[48] B. Silvi, J. Mol. Struct. 2002, **614**, 3-10. https://doi.org/10.1016/S0022-2860(02)00231-4

[49] S. Noury, F. Colonna, A. Savin and B. Silvi, *J. Mol. Struct.,* 1998, **450**, 59-68. https://doi.org/10.1016/S0022-2860(98)00413-X

[50] S. Shaik, D. Danovich, B. Silvi, D. L. Lauvergnat and P. C. Hiberty, Chem. Eur. J. 2005, **11**, 6358–6371. https://doi.org/10.1002/chem.200500265

[51] S. Raub and G. A. Jansen, *Theor. Chem. Acc.,* 2001, **106**, 223–232. https://doi.org/10.1007/s002140100268